

Growth of potassium tantalate (KTaO₃) crystals by directional solidification

Toshinori Taishi*, Takayuki Takenaka, Kazuya Hosokawa, Noriko Bamba, Keigo Hoshikawa

Faculty of Engineering, Shinshu University, 4-17-1, Wakasato, Nagano 380-8553, Japan

Potassium tantalate (KTaO₃) crystals were grown by directional solidification from various compositions of K₂CO₃-Ta₂O₅ melt. When raw materials with the stoichiometric composition (K₂CO₃:Ta₂O₅ = 50:50 mol%) were used, K₆Ta_{10.8}O₃₀ crystallized as the primary phase, indicating that KTaO₃ melts incongruently. K₆Ta_{10.8}O₃₀ is newly found in the K₂CO₃-Ta₂O₅ phase diagram and it is stably synthesized at temperatures above 1200 °C. In contrast, KTaO₃ crystallized when the ratio of K₂CO₃ was more than 51.5 mol%. There were three kinds of color in the KTaO₃-crystallized portions: milky white, colorless transparent and pale yellow. Based on these results, the phase diagram of the K₂CO₃-Ta₂O₅ system around the stoichiometric composition of KTaO₃ is proposed.

Keywords: A1: Directional solidification, A2: Growth from solutions, B1: Oxide, B1: Potassium compounds, B2: Nonlinear optic materials

* Corresponding author: Toshinori Taishi

Phone: +81-26-269-5383, FAX: +81-26-269-5383

E-mail: taishi@shinshu-u.ac.jp

Affiliation: Faculty of Engineering, Shinshu University

Address: 4-17-1, Wakasato, Nagano 380-8553, JAPAN

1. Introduction

Potassium tantalate (KTaO_3) is known as a colorless-transparent crystal. It has a high refractive index of 2.38 [1], similar to that of diamond, but has a suitable hardness for easy processing, similar to that of glass. Therefore, applications such as ball-shaped lenses for optical disk systems are expected [1]. KTaO_3 is a cubic perovskite structure but has no ferroelectric properties [2], i.e. it does not have any Curie point, while similar structure materials such as potassium niobate (KNbO_3) and potassium tantalite niobate ($\text{KTa}_{1-x}\text{Nb}_x\text{O}_3$: KTN) have ferroelectricity [2-4].

According to the K_2CO_3 - Ta_2O_5 phase diagram [5], the liquidus and solidus close to the ratio of K_2CO_3 : $\text{Ta}_2\text{O}_5 = 50$: 50 mol% (stoichiometric composition for KTaO_3) have not been reported precisely. Although the primary phase for the stoichiometric melt has been reported to be KTaO_3 [5], KTaO_3 has been recognized as an incongruent material. In fact, KTaO_3 crystal is generally grown by solution growth such as top-seeded solution growth (TSSG) [1], the flux method [6] or the hydrothermal technique [7]. The crystal shape grown is rectangular, reflecting the crystal structure. The size of crystals grown by the flux method and the hydrothermal technique is about 2 – 4 mm [6,7]. The growth rate of KTaO_3 crystals grown by such solution growth was approximately 0.05 – 0.1 mm/h.

In our previous study [8], with regard to incongruent KNbO_3 , crystals were

grown by directional solidification, and it was found that KNbO_3 crystals crystallized from the melt with the composition of K_2CO_3 between 51 and 52 mol%. Then, KNbO_3 crystals were successfully grown by the vertical Bridgman (VB) technique using a seed and raw materials with this K-rich composition [9].

In the present study, KTaO_3 crystals were grown by directional solidification from melts with various compositions of K_2CO_3 - Ta_2O_5 , and the melt composition for which KTaO_3 crystallizes as the primary phase was investigated. From the results, a new compound was found as the primary phase from the stoichiometric KTaO_3 melt. According to these results, the phase diagram of K_2CO_3 - Ta_2O_5 system around the stoichiometric composition was investigated.

2. Experimental procedure

Powders of K_2CO_3 (purity 99.9%) and Ta_2O_5 (99.99 %) were used as starting materials and these powders were mixed in ethanol for 24 hours at ratios of K_2CO_3 to $\text{Ta}_2\text{O}_5 = 50:50$ (stoichiometric composition), 51.0:49.0, 51.5:48.5 and 52.0:48.0 mol%. The mixture was calcined at 800°C for 3 hours in air after being dried and compressed, and the cylindrical compounds so obtained were used as the raw materials. These raw materials were used to charge in a cylindrical platinum crucible with an inner diameter of 20 mm. The crucible was set on an alumina support in a furnace after a platinum lid

had been put on the crucible. The temperature gradient upon seeding was 10 - 12°C/cm and the rotational speed of the crucible was 6 rpm. After the raw materials had melted completely, the crucible was pulled down at a rate of 0.5 mm/h, and the crystals were grown by directional solidification in air. The growth apparatus and detailed growth conditions have been reported previously [10]. The crystal was cooled to room temperature for 16 hours after the completion of the crystal growth, and the platinum crucible was peeled away and removed from the crystal. The As-grown crystal surface was examined using an optical microscope. The phase identification in the grown crystal was determined by powder X-ray diffraction (XRD) using RINT2200V/PC (RIGAKU). The composition of the grown crystals was evaluated by electron probe microanalysis (EPMA) using EPMA-1610 (SHIMADZU).

3. Results and discussion

3.1 The primary phase from the melt with close to the stoichiometric composition of KTaO_3

Figure 1 shows a photograph of a boule directionally solidified using raw materials in the ratio of K_2CO_3 : $\text{Ta}_2\text{O}_5 = 50:50$. The boule consists of three regions, A, B and C, as labeled in the figure. In the initial solidification region A,

many needle-like compounds were observed on the lower surface as may be seen in the optical micrograph as indicated white arrows shown in Fig. 2. The vertical length of region A was 5 mm. The neighboring region, B, which was 44mm in length, was a milky white polycrystalline structure with a grain size of several millimeters. The final solidification stage, region C, consisted of hygroscopic white alkaline products.

Figure 3 shows a back-scattered electron image of a wafer cut from region A. Two kinds of compounds were observed, one being the matrix labeled (a) and the other being the light-gray-colored needle-like compound labeled (b). The lighter color of compound (b), compared with compound (a), indicates that the composition of Ta in compound (b) is higher than that in the matrix. Indeed, the compositions of K and Ta in compounds (a) and (b) analyzed by EPMA were 48.0 and 52.0 mol% respectively for compound (a) and 34.4 and 65.6 mol% respectively for compound (b).

A part of region A and a part of region B in the boule were crushed into powder, and the phase identification of each region determined by XRD. Figure 4 shows the results of XRD for regions A and B shown in Fig. 1. The results of the XRD investigation revealed that region A consisted of a mixture of $K_6Ta_{10.8}O_{30}$

and KTaO_3 , while region B was pure KTaO_3 . The results for region A is consistent with the EPMA analysis, that is, compounds (a) and (b) in Fig. 3 corresponded to KTaO_3 and $\text{K}_6\text{Ta}_{10.8}\text{O}_{30}$, respectively. From these results, it was confirmed that KTaO_3 melts incongruently and $\text{K}_6\text{Ta}_{10.8}\text{O}_{30}$ crystallized as the primary phase of the stoichiometric KTaO_3 melt.

According to the phase diagrams of the $\text{K}_2\text{CO}_3\text{-Ta}_2\text{O}_5$ system reported by Reisman et al. [5], when stoichiometric KTaO_3 melt is cooled, $\text{K}_2\text{Ta}_4\text{O}_{11}$ should crystallize as the primary phase. $\text{K}_6\text{Ta}_{10.8}\text{O}_{30}$ compound, as detected in the present study, was not shown in the phase diagram. In order to confirm whether such a compound is formed stably or not, specimens calcined at 800, 1000 and 1200 °C for 10 h were prepared from the mixture of K_2CO_3 and Ta_2O_5 in the ratio of 35.7:64.3 mol%, which corresponds to the ratio of $\text{K}_6\text{Ta}_{10.8}\text{O}_{30}$. The detailed procedure was similar to that described above for making raw materials. Figure 5 shows XRD patterns for specimens calcined at each temperature. From XRD analysis, it was found that $\text{K}_2\text{Ta}_4\text{O}_{11}$ and KTaO_3 were detected for the material which had been calcined at 800 °C. $\text{K}_2\text{Ta}_4\text{O}_{11}$ and $\text{K}_6\text{Ta}_{10.8}\text{O}_{30}$ were detected for 1000 °C, while only $\text{K}_6\text{Ta}_{10.8}\text{O}_{30}$ was detected for 1200 °C. These indicate that $\text{K}_6\text{Ta}_{10.8}\text{O}_{30}$ compound is formed stably with the K_2CO_3 composition of 35.2 mol% between

33.3 mol% for $K_2Ta_4O_{11}$ and 50 mol% for $KTaO_3$ at temperatures above 1200 °C.

3.2 Melt composition for growing $KTaO_3$ crystal as the primary phase and the detailed phase diagram of K_2CO_3 - Ta_2O_5 close to $KTaO_3$ melt

Figures 6 (a) - (c) show photographs of three boules directionally solidified using raw materials with the ratio of K_2CO_3 : Ta_2O_5 = 51.0:49.0 mol %, 51.5:48.5 mol % and 52.0:48.0 mol %, respectively. In the case of the ratio of K_2CO_3 : Ta_2O_5 = 51.0: 49.0 mol%, region A including $K_6Ta_{10.8}O_{30}$ appeared at the bottom of the boule, then the $KTaO_3$ of the region B was observed as shown in Fig. 6 (a). Region B can be visually separated into three regions, B1, B2 and B3. First, milky white $KTaO_3$ crystallized in region B1, then, colorless-transparent $KTaO_3$ crystallized in region B2, and the third pale-yellow $KTaO_3$ crystallized in region B3. Finally, white alkaline products appeared in region C. In contrast, region A could not be observed in boules grown using raw materials with the ratio of K_2CO_3 : Ta_2O_5 = 51.5:48.5 mol % and 52.0:48.0 mol % as shown in Figs. 6 (b) and (c), respectively. The $KTaO_3$ of region B was observed from the bottom of boules, and it can be separated similarly into B1, B2 and B3, then finally region C appeared. These indicate that the K composition in the melt for growing $KTaO_3$

exists in the range from 51.5 to 67.7 mol%. In addition, region B2, corresponding to colorless-transparent KTaO_3 appears lower with increasing composition of K_2CO_3 in the raw material. This implies that there is a suitable melt composition range for crystallization of colorless-transparent KTaO_3 at the K composition between 51.5 and 67.7 mol%. This was consistent with the growth condition for growing a colorless-transparent KTaO_3 crystal by TSSG method [11].

On the basis of these observed results, the existence of non-stoichiometry in KTaO_3 is clarified, which is similar to the case of KNbO_3 . A schematic phase diagram around the KTaO_3 phase in the $\text{K}_2\text{CO}_3\text{--Ta}_2\text{O}_5$ system is deduced as shown in Fig. 7, although the melting temperature of the $\text{K}_6\text{Ta}_{10.8}\text{O}_{30}$ was not measured in the present study. When stoichiometric KTaO_3 melt is cooled, it decomposes into $\text{K}_6\text{Ta}_{10.8}\text{O}_{30}$ and liquid (region A) due to its incongruently. Furthermore, KTaO_3 crystallizes at the melt composition of K_2CO_3 between 51.5 and 67.7 mol% (region B). In this portion there are three-colored regions, milky white, colorless-transparent and pale-yellow. There is probably a narrow solid solution range of the KTaO_3 phase, resulting in crystallization of KTaO_3 with three different colors. Detailed classification according to the melt composition is now in progress. Finally white hygroscopic alkaline compounds crystallize at the

eutectic composition of 67.7 mol%. According to the reported phase diagram, such compound in region C is a mixture of KTaO_3 and K_3TaO_4 .

Based on the present investigation, a KTaO_3 single crystal will be grown by the VB technique using high-quality seed from a K-rich melt (higher than 51.5 mol%), in a case similar to that of KNbO_3 [8,9]. After growing KTaO_3 single crystals, the mechanism of the color change in a KTaO_3 crystal due to the composition of K_2CO_3 in the melt will be clarified using high quality crystals. Such advanced study is now in progress, and results will be reported elsewhere.

4. Conclusion

KTaO_3 crystals were grown by directional solidification from various compositions of K_2CO_3 - Ta_2O_5 melt, and the grown crystals were evaluated. When raw materials with the stoichiometric composition (K_2CO_3 : Ta_2O_5 = 50:50 mol%) was used, $\text{K}_6\text{Ta}_{10.8}\text{O}_{30}$ crystallized as the primary phase. This indicates that KTaO_3 melts incongruently. $\text{K}_6\text{Ta}_{10.8}\text{O}_{30}$ is newly found as a compound with the composition of K_2CO_3 between 33.3 mol% ($\text{K}_2\text{Ta}_4\text{O}_{11}$) and 50 mol% (KTaO_3). On the other hand, KTaO_3 crystallized when the ratio of K_2CO_3 was more than 51.5 mol% without crystallization of $\text{K}_6\text{Ta}_{10.8}\text{O}_{30}$. There were three kinds of color in KTaO_3 -crystallized portions, milky white, colorless transparent and pale yellow.

Based on these experimental results, a phase diagram around the KTaO_3 compound in the K_2CO_3 – Ta_2O_5 system is proposed. Such results will be useful for growing KTaO_3 crystals by the VB technique using a KTaO_3 seed.

Acknowledgement

This work was supported in part by an Adaptable and Seamless Technology transfer Program through targetdrive R&D (A-STEP: AS2315011C) from the Japan Science and Technology Agency.

References

- [1] K. Fujiura, M. Sasaura, KTaO₃ Solid Immersion Lens for Nearfield Optical Disk System, NTT Technical Review **5** (2007) 1-5.
- [2] D. Rytz, H. J. Scheel, Crystal Growth of KTa_{1-x}Nb_xO₃ (0<x<0.04) Solid Solutions by a Slow-Cooling Method, Journal of Crystal Growth **59** (1982) 468-484.
- [3] B. T. Matthias, J. P. Remeika, Physical Review **82** (1951) 727.
- [4] S. Triebwasser, Study of Ferroelectric Transitions of Solid-Solution Single Crystals of K₂O₃-KTaO₃, Physical Review **114** (1959) 63-70.
- [5] A. Reisman, F. Holzberg, M. Berkenblit, M. Berry, Reaction of the Group VB Pentoxide with Alkali Oxides and Carbonates. III. Thermal and X-ray Phase Diagrams of the System K₂O or K₂CO₃ with Ta₂O₅, Journal of American Chemical Society **78** (1956) 4514-4520.
- [6] S. Zlotnik, P. M. Vilarinho, M. E. V. Costa, J. A. Moreira, A. Almeida, Growth of Incipient Ferroelectric KTaO₃ Single Crystals by a Modified Self-Flux Solution Method, Crystal Growth & Design **10** (2010) 3397-3404.
- [7] M. Mann, S. Jackson, J. Kolis, Hydrothermal crystal growth of the potassium niobate and potassium tantalite family of crystals, Journal of Solid State

Chemistry **183** (2010) 2675-2680.

- [8] K. Kudo, K. Kakiuchi, K. Mizutani, T. Fukami, K. Hoshikawa, Non-stoichiometry in potassium niobate crystals grown by directional solidification, *Journal of Crystal Growth* **267** (2004) 150–155.
- [9] K. Kudo, K. Kakiuchi, N. Endo, N. Bamba, K. Hoshikawa, T. Fukami, *Japanese Journal of Applied Physics* **43** (2004) 6701-6705.
- [10] T. Taishi, T. Hayashi, T. Fukami, K. Hoshikawa, I. Yonenaga, Single-crystal growth of langasite ($\text{La}_3\text{Ga}_5\text{SiO}_{14}$) by the vertical Bridgman (VB) method in air and in an Ar atmosphere, *Journal of Crystal Growth* **304** (2007) 4–6.
- [11] M. Kamoshita, H. Ishii, H. Yamamoto, K. Mochizuki, S. Kawanami, Single Crystal Growth of KTaO_3 by the TSSG Method, *Journal of Flux Growth* **5** (2010) 83. [in Japanese]

Figure captions

Fig. 1 A photograph of a boule directionally solidified from melt with a ratio of K_2CO_3 :
 $\text{Ta}_2\text{O}_5 = 50: 50$ mol%.

Fig. 2 Optical micrograph of the lower surface of region A in the boule shown in Fig. 1.
White arrows indicate the needle-like compound.

Fig. 3 Back-scattered electron image of a wafer cut from region A shown in Fig. 1.

Fig. 4 Powder XRD patterns of region A and B of the boule shown in Fig. 1.

Fig. 5 Powder XRD patterns of compounds calcined from a mixture of K_2CO_3 and
 Ta_2O_5 with a ratio of 35.7: 64.3 mol% at 800, 1000 and 1200 °C. Standard peaks of
three corresponding compounds are also shown.

Fig. 6 Photographs of boules directionally solidified from melt with a K_2CO_3 : Ta_2O_5
ratio of (a) 51.0:49.0 mol %, (b) 51.5:48.5 mol% and (c) 52.0:48.0 mol%.

Fig. 7 Schematic illustration of phase diagram of $\text{K}_2\text{CO}_3\text{--Ta}_2\text{O}_5$ system with a K_2CO_3 composition of between 32 and 68 mol%.



Fig. 1

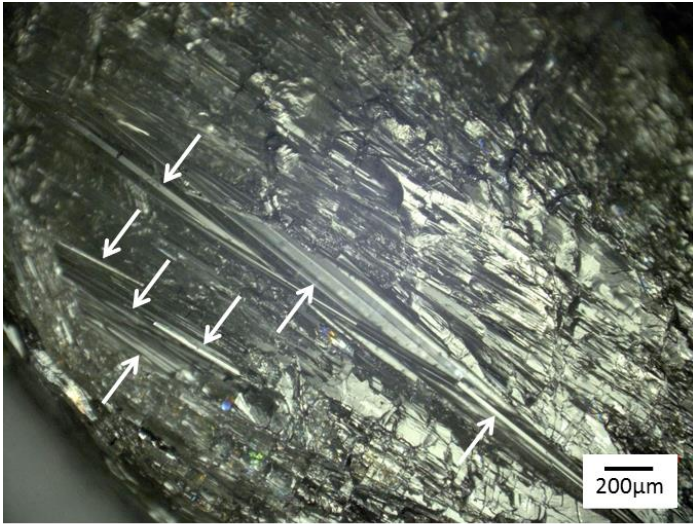
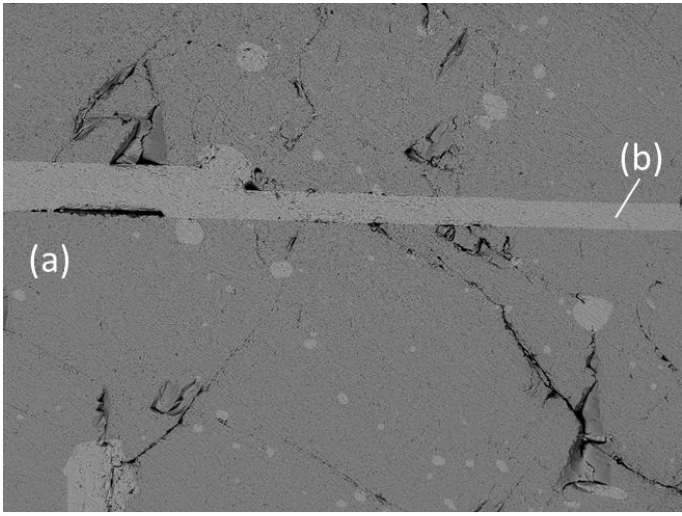


Fig. 2



100um

Fig. 3

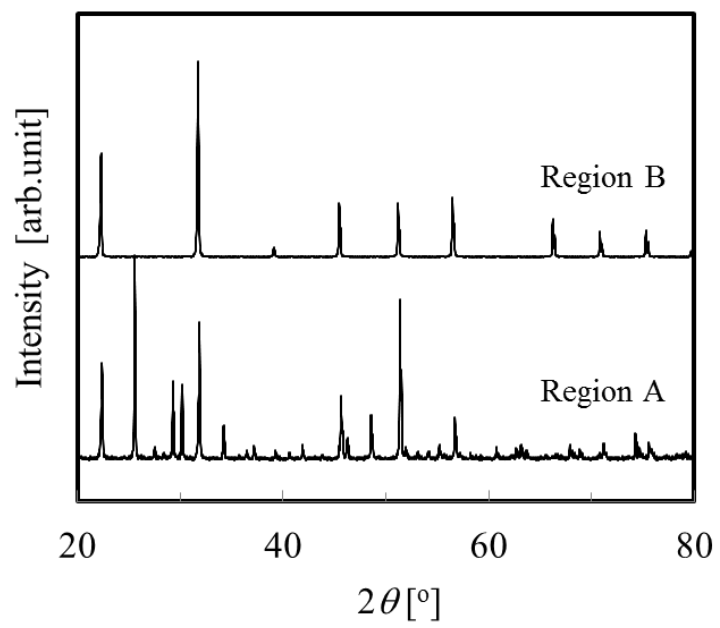


Fig. 4

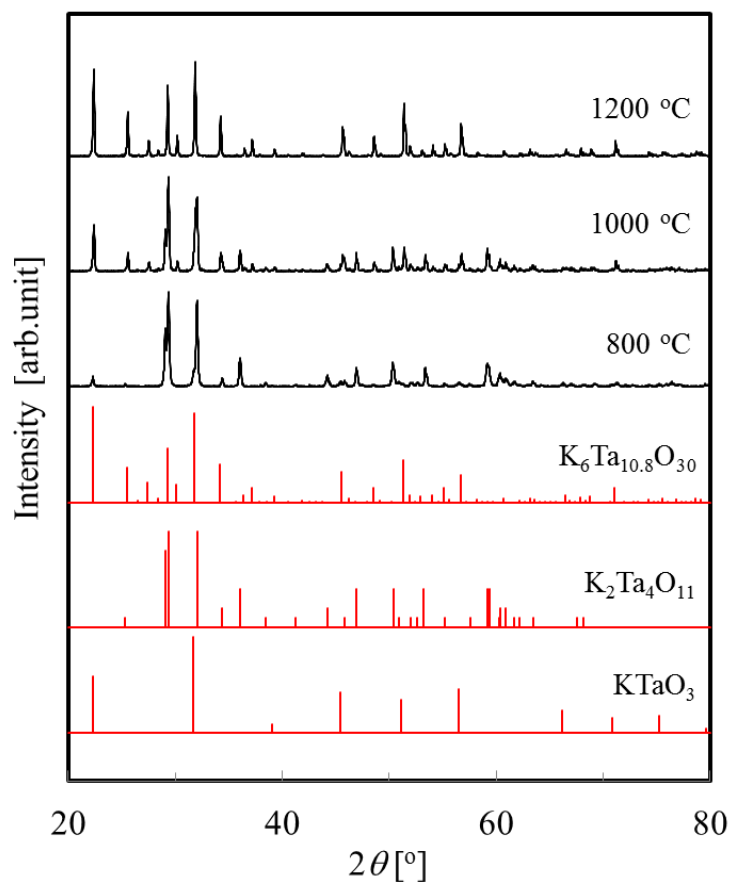


Fig. 5

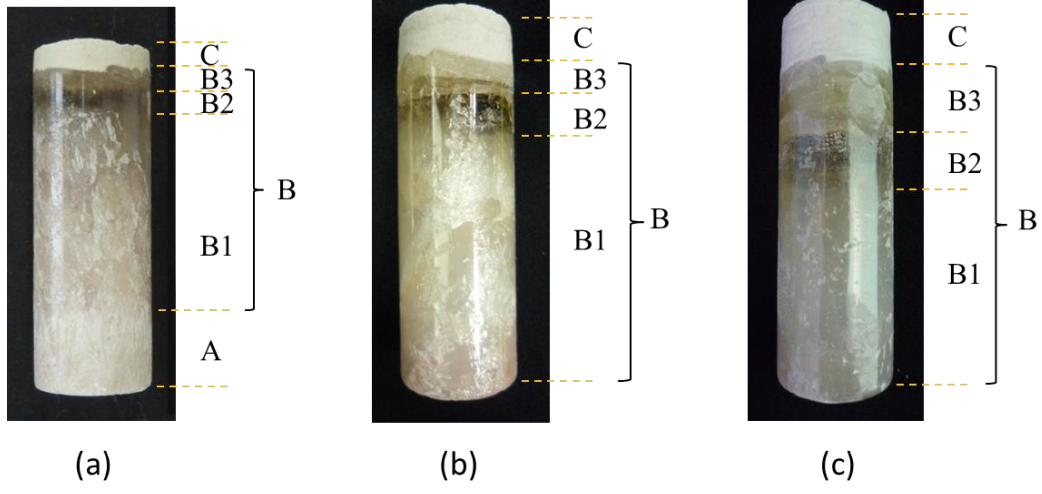


Fig. 6

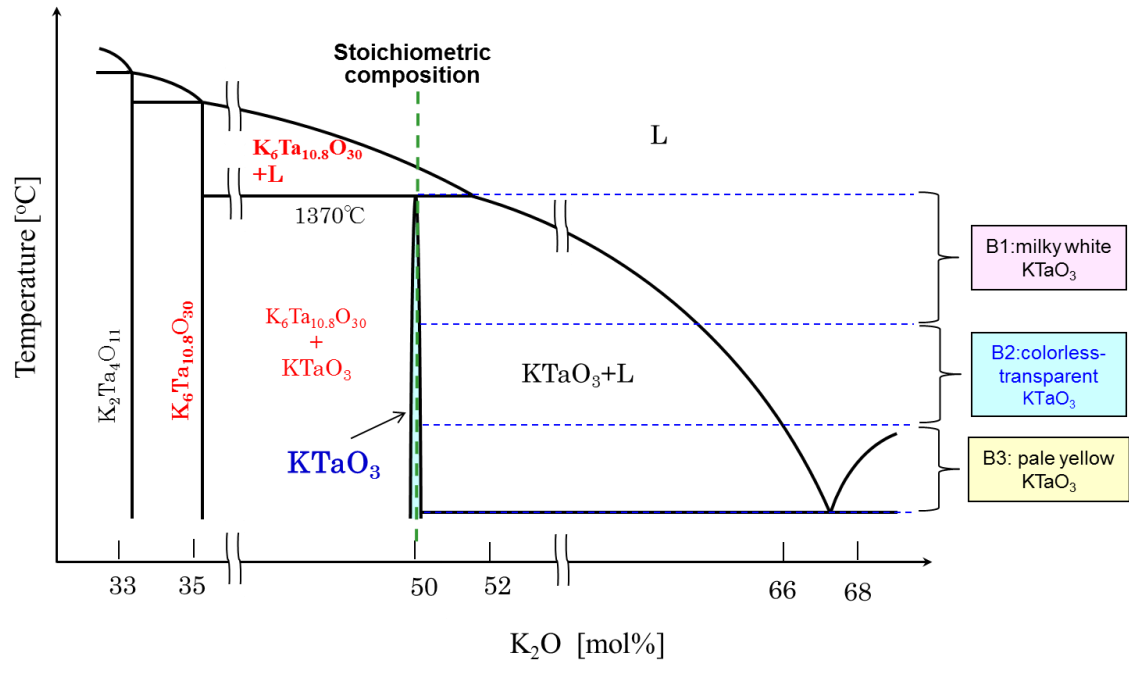


Fig. 7